ISSN: 0975-8585

Research Journal of Pharmaceutical, Biological and Chemical Sciences

Spectral characterization and DFT Computational studies on (*E*)-*N*′-(4-chlorobenzylidene)-4-chlorobenzenesulfonohydrazide.

Akshatha R Salian[1,2]*, B Thimme Gowda[2], Vishalakshi B[2], Sabine Foro[3], and S Meenakshisundaram[4].

[1]Department of Chemistry, School of Physical Sciences, St Aloysius (Deemed to be University) Mangaluru, 575003, Karnataka, India.
[2]Department of Chemistry, Mangalore University, Mangalagangotri-574199, Mangalore, India.
[3]Institute of Materials Science, Darmstadt University of Technology, Alarich-Weiss-Str. 2, D-64287, Darmstadt, Germany.
[4]Department of Chemistry, Annamalai University, Annamalainagar – 608002, Tamilnadu, India.

ABSTRACT

The compound, (*E*)-*N*′-(4-chlorobenzylidene)-4-chlorobenzenesulfonohydrazide, N4CB4CBSH has been synthesized and characterized by FT-IR, ^{1}H and ^{13}C NMR spectroscopic techniques. The density functional theoretical computation method has been used for HOMO-LUMO analysis to calculate the energy gap and related molecular properties and also, the HOMO-LUMO investigations are matched with the calculated UV-Visible spectrum. Further, the molecular electrostatic potential (MEP), the first-order hyperpolarizability (β) and dipole moment (μ) were also computed using B3LYPG/6-31G method. Mulliken charge population analysis is used to obtain the atomic charge distributions on different atoms of the molecule. The intermolecular interactions observed in the crystal packing of the compound have been discussed by using MEP surface generated and Mulliken charge population computed.

Keywords: Schiff base, DFT, FMO, Mulliken charge population analysis, hyperpolarizability, MEP.

https://doi.org/10.33887/rjpbcs/2025.16.5.11

Corresponding author

ISSN: 0975-8585

INTRODUCTION

Schiff bases are the class of organic compounds possessing broad spectrum of biological activities [1-8] along with many other interesting properties such as magnetic properties [9-10]. The imine group (-N=CH-) present in the Schiff base molecules is responsible for their biological activities [11]. Schiff bases are capable of forming complexes with metal ions to produce mononuclear and also polynuclear metal complexes [12-13]. In colorimetric or fluorometric analysis, Schiff bases find good application as multidentate ligands for the transition metal ions [14-15]. Due to the delocalisation of π-electron clouds over the molecules, Schiff bases show large molecular hyperpolarizability (β) and hence attracted the researcher's attention to investigate their nonlinear optical (NLO) properties [16-17]. The spectroscopic and density functional theory (DFT)-based computational studies of the NLO crystal (*E*)-*N*′-(4-chlorobenzylidene)-4-methylbenzenesulfonohydrazide has been studied [18]. The study suggested the superior NLO response of the compound compared to urea, the organic prototypical molecule. The study also revealed that the substitution of chlorine with bromine showed better NLO response. In our paper, the crystal structure, Hirshfeld surface analysis of N4CB4CBSH has been discussed in detail [19]. The compound is crystallized in triclinic crystal system with $P\bar{1}$space group possessing one molecule in the asymmetric unit with the unit cell parameters of a = 5.9306(6) Å, b = 9.477(1) Å, c = 13.040(2) Å, α = 98.822(9)°, β = 96.046(9)°, γ = 92.416(9)°, V = 718.94(15) $Å^3$ and Z = 2 (Figure 1). The configuration of the molecule about the C=N bond and the various intermolecular hydrogen bond interactions are confirmed. In the present study, we report the frontier molecular orbital (FMO) analysis, first-order molecular hyperpolarizability, Mulliken charge population analysis and MEP of the title compound using DFT studies in order to explore structural properties of the compound further.

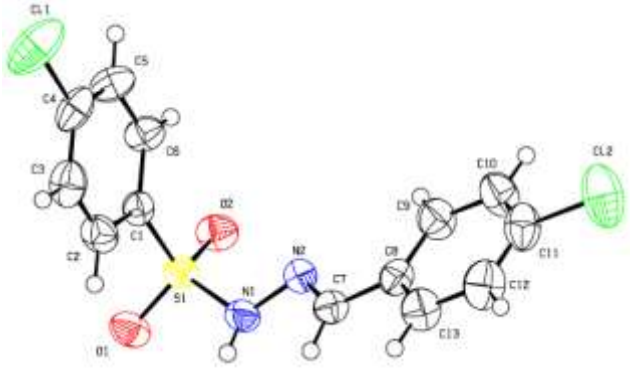

Figure 1: The asymmetric unit of the title compound N4CB4CBSH

EXPERIMENTAL

Synthesis of N4CB4CBSH and Instrumentation for spectral characterization

Synthesis of the title compound, N4CB4CBSH (Figure 2) has been described in our paper [20]. The compound is characterized by FT-IR spectroscopy recorded in KBr pellets on a Shimadzu FT-IR 157 spectrometer in the frequency range 400 - 4000 cm^{-1}. The NMR spectrum of the compound was measured on a BRUKER AVANCE II 400MHz FT NMR spectrometer. The spectrum was recorded in DMSO with tetramethylsilane (Me_4Si) as internal standard. Computational studies were done using the GAUSSIAN 09 software using the DFT.

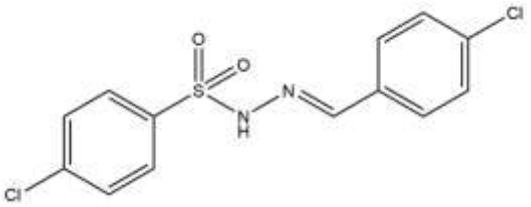

Figure 2: Chemical structure of (*E*)-*N*′-(4-chlorobenzylidene)-4-chlorobenzenesulfonohydrazide, N4CB4CBSH

ISSN: 0975-8585

RESULTS AND DISCUSSION

Fourier transform infrared (FT-IR) spectrum

The characteristic vibrational bands observed in the FT-IR spectrum of N4CB4CBSH are shown in Figure 3. The S=O asymmetric and symmetric stretching vibrations are observed at 1327.0 and 1168.9 cm^{-1}, respectively. The C=N stretching vibration is observed at 1583.6 cm^{-1} and the N-H stretching vibration at 3180.6 cm^{-1}. Table 1 lists various modes of vibrations in the molecule and their respective vibrational frequencies.

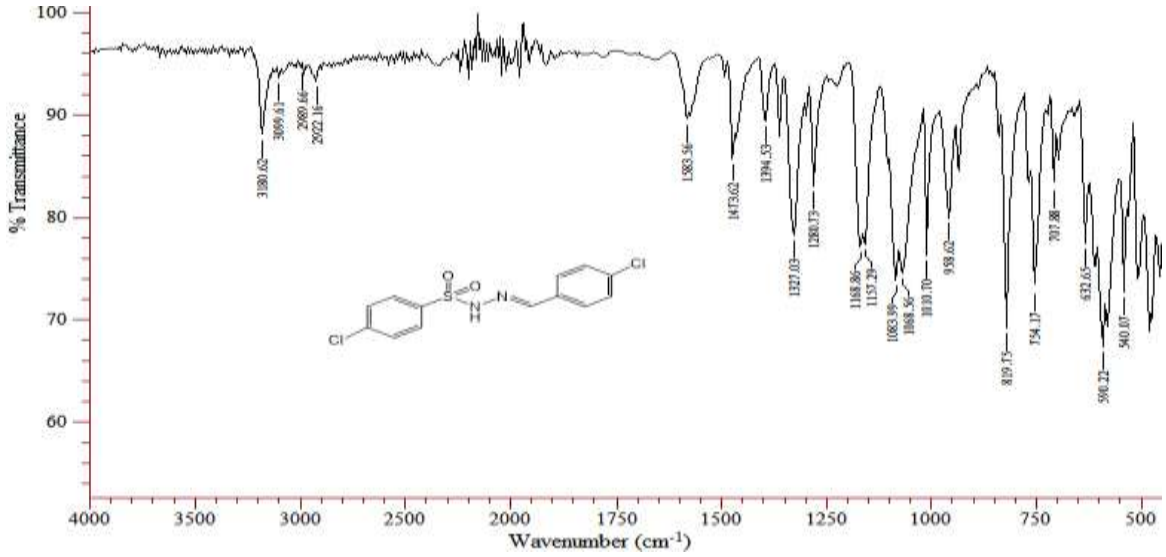

Figure 3: Experimental FT-IR spectrum of N4CB4CBSH.

Table 1: Different modes of vibrations and their vibrational frequencies in N4CB4CBSH.

Mode of vibration	Vibrational frequency (cm^{-1})
N-H (asym str)	3180.6 s
C-H (Ar sym str)	3099.6 w
C-H (imine str)	2922.2 w
C=N(str)	1573.6 m
C=C (Ar in plane str)	1473.6 m
S=O (asym)	1347.8 s
S=O (sym)	1168.9 s
C-H (Ar in plane bend)	1085.9 w
S-N (sym str)	958.6 w
C-S (str)	819.8 m
C-Cl (str)	754.2 s

s = strong, m = medium, w = weak

Nuclear magnetic Resonance (^1H and ^{13}C NMR) spectra

The ^1H NMR spectrum of N4CB4CBSH is shown in Figure 4. ^1H NMR (400 MHz, DMSO-d_6): δ = 7.32 (d, 2H, J = 8.4Hz, Ar-H), 7.52 (dd, 4H, Ar-H, J = 8.76 and 2.56 Hz), 7.87 – 7.92 (m, 3H; 2 Ar-H & 1 =C-H) and 11.50 (s, 1H, N-H).

ISSN: 0975-8585

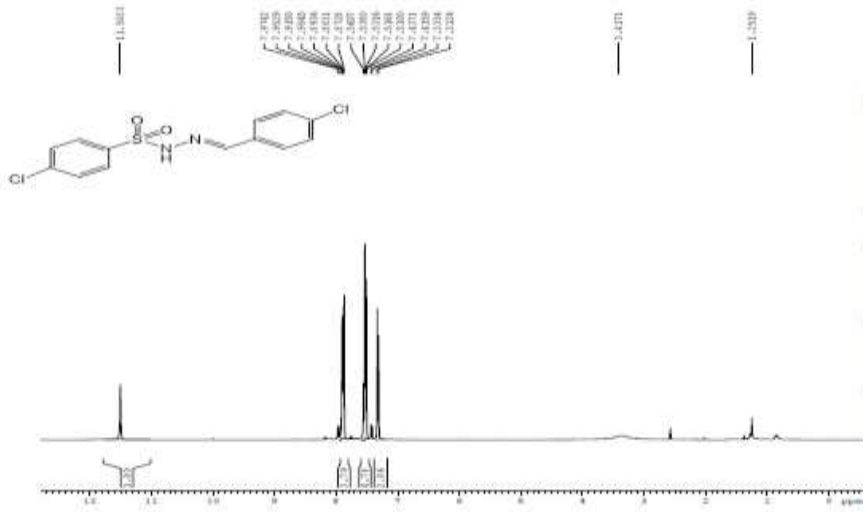

Figure 4: Experimental ^{1}H NMR spectrum of N4CB4CBSH

The ^{13}C NMR spectrum of N4CB4CBSH is shown in Figure 5.

^{13}C NMR (100 MHz, DMSO-d6): δ = 128.38, 129.42, 130.73, 132.06, 134.96, 137.47, 138.39, 139.32, 145.66.

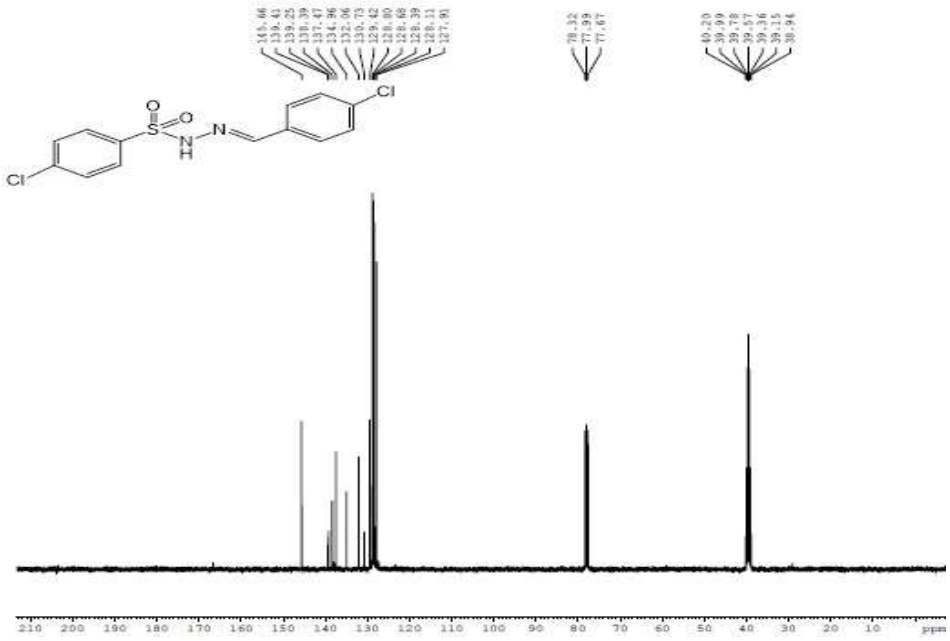

Figure 5: Experimental ^{13}C NMR spectrum of N4CB4CBSH

Computational results

Frontier Molecular Orbital Energy Analysis

The electronic spectrum of N4CB4CBSH was calculated by CIS method using the B3LYP density functional in the gas phase. The representative spectrum is given in Figure 6. The strong and the sharp band at 215.66 nm (λ_{max}) with the oscillator strength of 0.7106 corresponds to π→π* transitions in the molecule. HOMO (highest occupied molecular orbital), LUMO (lowest unoccupied molecular orbital) and the band gap energy in N4CB4CBSH molecule has been calculated by B3LYP/6-311(d,p) method. The HOMO and LUMO indicate the ability of a molecule to donate and accept the electrons, respectively [21]. The electronic

structure of the molecules is characterized by the HOMO-LUMO gap energy. It is the index of both electrical conductivity and chemical reactivity [22].

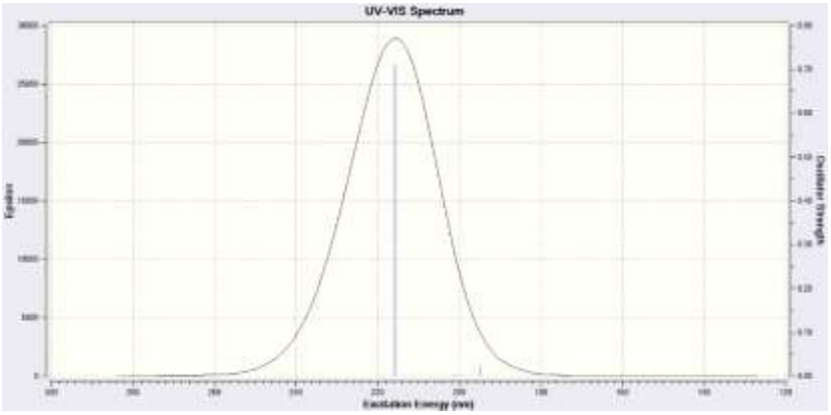

Figure 6: Simulated electronic spectrum of N4CB4CBSH

Figure 7 shows HOMO-LUMO plot and their band gap energy of 4.851 eV, confirms the stable structure of the molecule. The positive and negative values of the wave function is represented by the red and green colours, respectively. HOMO and LUMO energy values of a molecule can be used to calculate various other molecular properties. Electronegativity is the power of an atom of a compound to attract the electrons towards it. The electronegativity and electronic chemical potential can be calculated by the values of electron affinity and ionisation energy as, $\chi = [(I + A)/2]$ and $\mu = -1/2(I+A)$, respectively. HOMO-LUMO energy gap is directly related to the hardness of a molecule and it reflects the stability of the molecule [23]. The global hardness, $\eta = 1/2(I- A)$. Electrophilic power of the molecule; Electrophilicity index, ω can be calculated from the values of chemical potential and global hardness as $\omega = \mu^2/2\eta$. Chemical Softness, $S = 1/2\eta$ is the measure of chemical reactivity of the molecule. The magnitude of various properties of the molecule as shown in Table 2, are highly significant in predicting the biological activities.

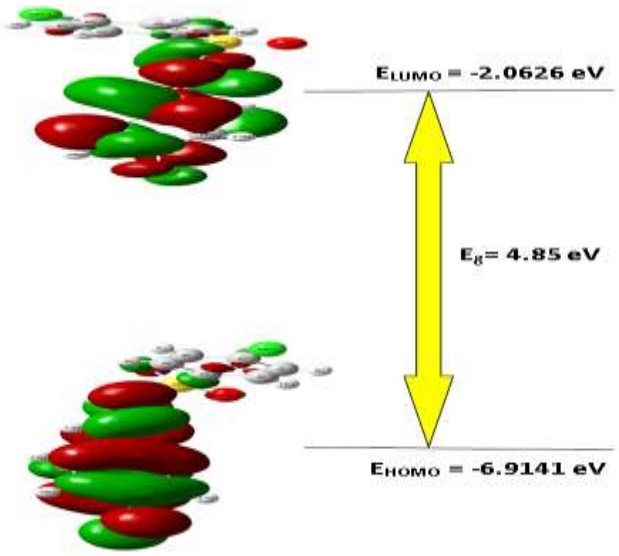

Figure 7: The frontier molecular orbital diagram of N4CB4CBSH

ISSN: 0975-8585

Table 2: Calculated energy values of N4CB4CBSH by B3LYP/6-311G method.

Molecular energy	Values (eV)
E_{HOMO}	-6.914
E_{LUMO}	-2.063
HOMO-LUMO energy gap	4.851
Ionization potential, I	6.914
Electron affinity, A	2.063
Electronegativity, χ	4.488
Chemical potential, μ	-4.488
Chemical Hardness, η	2.428
Chemical Softness, S	0.206
Electrophilicity index, ω	4.152
overall energy balance, ΔE	-4.852

Non-Linear Optical (NLO) properties

Due to the electron delocalization in the π-π* orbitals of the organic compounds, they are expected show comparatively good optical properties. The calculated values for the first order hyperpolarizability (β) and the dipole moment (μ) of N4CB4CBSH are given in Table 3.

Using the x, y, z components, the total dipole moment μ_{tot} and total first order hyperpolarizability β_{tot} can be calculated as:

$$\mu = (\mu_x^2 + \mu_y^2 + \mu_z^2)^{1/2} \quad (1)$$

and

$$\beta_{tot} = (\beta_x^2 + \beta_y^2 + \beta_z^2)^{1/2} \quad (2)$$

where,

$$\beta_x = \beta_{xxx} + \beta_{xyy} + \beta_{xzz} \quad (3)$$

$$\beta_y = \beta_{yyy} + \beta_{xxy} + \beta_{yzz} \quad (4)$$

$$\beta_z = \beta_{zzz} + \beta_{zxx} + \beta_{zyy} \quad (5)$$

Table 3: The calculated First-order molecular hyperpolarizability and Dipole moment of N4CB4CBSH

First-order molecular hyperpolarizability, β (10^{-30} e.s.u)	
β_{xxx}	-517.08329
β_{xxy}	-84.48012
β_{xyy}	7.52428
β_{yyy}	-211.85366
β_{xxz}	111.58313
β_{xyz}	66.98014
β_{yyz}	18.81626
β_{xzz}	-17.65045
β_{yzz}	24.02673
β_{zzz}	90.25945
β_{tot} (10^{-30} e.s.u)	5.4691
Dipole moment, μ (D)	
μ_x	0.52709
μ_y	1.36329
μ_z	1.47937
μ_{tot}	5.2860

The calculated first-order molecular hyperpolarizability (β) and dipole moment (μ) of the specimen are, 5.4691 X 10^{-30} e.s.u (~ 20 times that of urea) and 5.2860 D, respectively. It is interesting to observe that the strong inter- and intramolecular hydrogen bondings enhance the hyperpolarizability leading to micro level nonlinearity. It is clear from the Table 3 that the delocalization of electron cloud is

more along x direction because of its large contribution to βtot. The non-zero value of dipole moment and high value of β of N4CB4CBSH indicates that it as an effective NLO material.

Mulliken charge population analysis

As the atomic charges affect the electronic structure and the dipole moments of the molecules, the calculation of Mulliken atomic charges has become an important implication of quantum mechanical calculation to the chemical system [24]. The computed Mulliken atomic charges of all the atoms present in N4CB4CBSH are shown in Table 4. The result shows that, two oxygen atoms attached to a sulphur atom, two nitrogen atoms and all the carbon atoms show negative charges, representing the electron withdrawing nature which indicates their facile interaction with receptors sites positively charged parts. i.e., these are the sites for electrophilic attack in the molecule. The two chlorine atoms (C11 and C12), a sulphur atom and all the hydrogen atoms with positive charges are the nucleophilic attack sites.

Table 4: Mulliken atomic charges of all the atoms present in N4CB4CBSH

Atom	Mulliken Charge (eV)
C1	-0.342067
C2	-0.044685
H1	0.213931
C3	-0.024399
H2	0.221298
C4	-0.364700
C5	-0.023595
H3	0.224986
C6	-0.053790
H4	0.237356
C7	-0.059171
H5	0.180550
C8	-0.059533
C9	-0.088133
H6	0.217150
C10	-0.057130
H7	0.216099
C11	-0.350909
C12	-0.052765
H8	0.213588
C13	-0.168519
H9	0.197823
N1	-0.642477
H10	0.358735
N1	-0.077088
O1	-0.611251
O2	-0.576353
Cl1	0.020355
Cl2	0.001024
S1	1.293671

The magnitude of negative charge on the carbon atoms vary significantly. The charge on N1 is more negative than the N2. The most negative charge containing Nitrogen atom (N1) attached to a hydrogen atom implies the favourable site for H-bond formation. Among the chlorine atoms, the Cl1 is more positive than Cl2. These also indicate the probable site for hydrogen bond interactions (non-classical). These expectations for the hydrogen bond interactions in the molecule are clearly manifested in the crystal packing of the compound obtained by the X-ray diffraction studies. N1-H1···O1, C4-Cl1···Cg2 and C11-Cl2···Cg1 (Cg1 and Cg2 are the centroids of rings C1–C6 and C8–C13, respectively) having the symmetry codes: -x+1; -y+1; -z, x+1, y-1, z and -x, -y+1, -z+1, respectively. From the hydrogen bond geometry data, the variation of hydrogen bond length (bond lengths of 3.41 (1) and 3.65 (1) Å, involving Cl1 and Cl2, respectively) for the two non-classical interactions, indicates that there is a change in the magnitude of the

positive charges on two Cl atoms and this observation in turn is well supported by the Mulliken charge population analysis. A plot for Mulliken charge distribution on N4CB4CBSH is shown in Figure 8.

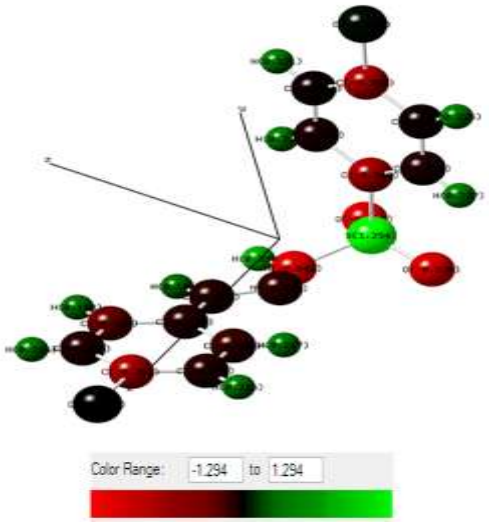

Figure 8: Plot of Mulliken atomic charge distribution for N4CB4CBSH

Mulliken charge population analysis can also be extended to support the data obtained from the Hirshfeld surface analysis of the molecule. The Hirshfeld surfaces mapped over d_{norm}, predicts the hydrogen bonding interactions. The bright red spots at the N-H and Oxygen atoms indicate the formation of strong hydrogen bond (N-H···O with H···O bong length of 2.07 (2) Å). Whereas, the weak interactions involving the chlorine atoms are indicated as light-red spots around the position of chlorine atoms in the molecule.

Molecular electrostatic potential

MEP is mapped over the stabilized geometry of the title compound, N4CB4CBSH. The electrostatic potential plays an important role in the discussion of the compounds chemical reactivity by identifying the sites of electrophilic and nucleophilic attack, the hydrogen bonding interactions and also the site of metallic bonding in the molecules [25].

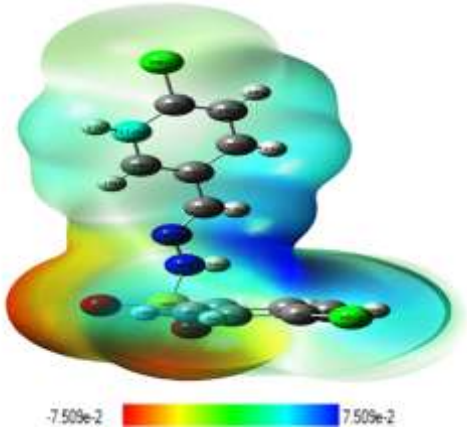

Figure 9: MEP plot of N4CB4CBSH.

The negative electrostatic potential region due to the lone pair of electrons and π-electrons is indicated by the red and yellow colour and these regions indicate the site of electrophilic reactivity. Positive electrostatic potential region where the nuclear charge density is incompletely shielded is represented by the blue colour and these regions indicate the sites of nucleophilic attack. The MEP plot depicting the relative polarity of the molecule is given in Figure 9. From the figure it is observed that the most electron rich sites of the molecular energy plot have been contributed by the oxygen atoms (most negative region)

of SO_2 group and the nitrogen atom (least negative region) of NH group. The region around H atoms attached nitrogen atom and azomethine carbon atom show highest positive potential sites (dark blue colour) followed by the two chlorine atoms (light blue colour).

CONCLUSION

The HOMO and LUMO energies were calculated and the HOMO-LUMO gap energy was found to be 4.851 eV, indicating good charge transfer within the molecule. Simulated UV-Visible spectral analysis revealed that the molecule has λ_{max} at 215.66 nm. The charges on atoms changed depending on their polarizability in the molecule and hence Mulliken charge population analysis gives an insight into the possibilities of hydrogen bonding interactions. The calculated MEP indicated the preferential sites of chemical reactivity in the molecule. From the MEP surface, it would be predicted that at the oxygen atoms, an electrophilic attack occurs preferentially, followed by the nitrogen atom of NH group. Whereas, the nucleophilic attack would preferentially occur at the hydrogen atoms of NH group followed by the hydrogen atom of azomethine moiety. The calculated NLO property, namely the first-order hyperpolarizability (β) value of the molecule indicates the molecule to be a good NLO material with potential for future studies.

REFERENCES

[1] Rafat M, Fleita DH, Sakka OK. Molecules 2011; 16: 16–27.
[2] da Silva CM, da Silva DL, Modolo LV, Alves RB, de Resende MA, Martins CVB, de Fatima A. J Adv Res 2011; 2: 1–8.
[3] Kumar KS, Ganguly S, Veerasamy R, De Clercq E. Eur J Med Chem 2010; 45: 5474–5479.
[4] Gungor O, Gurkan P. J Mol Struct 2014; 1074: 62–71.
[5] Pramanik HAR, Das D, Paul PC, Mondal P, Bhattacharjee CR. J Mol Struct 2014; 1059: 309–319.
[6] Bensaber SM, Allafe HA, Ermeli NB, Mohamed SB, Zetrini AA, Alsabri SG, Erhuma M, Hermann A, Jaeda MI, Gbaj AM. Med Chem 2014; 23: 5120–5134.
[7] Singh AK, Pandey SK, Pandey OP, Sengupta SK. J Mol Struct 2014; 1074: 376–383.
[8] Amer S, El-Wakiel N, El-Ghamry H. J Mol Struct 2013; 1049: 326–335.
[9] Liu WL, Zou Y, Li Y, Yao YG, Meng QJ. Polyhedron 2004; 23: 849–855.
[10] Murray KS. Adv Inorg Chem 1995; 43: 261–358.
[11] Arunagiri C, Subashini A, Saranya M, Muthiah PT, Thanigaimani K, Razak IA. Spectrochim Acta A 2015; 135: 307–316.
[12] Guerriero P, Tamburini S, Vigato PA. Coord Chem Rev 1995; 139: 17–243.
[13] Tarafder MTH, Jin KT, Crouse KA, Ali AM, Yamin BM, Fun HK. Polyhedron 2002; 21: 2547–2554.
[14] Terra LH, Areias AMC, Gaubeur I, Suez-Iha MEV. Spectrosc Lett 1999; 32: 271.
[15] Suez I, Pehkonen SO, Hoffmann MR. Sci Technol 1994; 28: 2080–2086.
[16] Karaka A, Elmali A, Unver H, Svoboda I. Spectrochim Acta A 2005; 61: 2979–2987.
[17] Unver H, Karaka A, Elmali A. J Mol Struct 2004; 702: 49–54.
[18] Sasikala V, Sajan D, Joseph L, Balaji J, Prabu S, Srinivasan P. Chem Phys Lett 2017; 674: 11–27.
[19] Salian AR, Foro S, Gowda BT. Acta Cryst E 2018; 74: 1808–1814.
[20] Salian AR, Foro S, Gowda BT. Acta Cryst E 2018; 74: 1613–1618.
[21] Becker H, Fleming J. J Für Prakt Chem 1978; 320: 879–880.
[22] Radovic LR, Bockrath B. J Am Chem Soc 2005; 127: 5917–5927.
[23] Sadekov ID, Minkin VI, Lutskii AE. Russ Chem Rev 1970; 39: 179–195.
[24] Sridher D, Muthusamy A, Kannappan V, Karunathan R, Sathyanarayanamoorthi V. Elixir Vib Spec 2014; 72: 25577–25582.
[25] Tanak H, Koçak F, Ağar E. Mol Phys 2016; 114: 197–212.